

Liquid-phase Knoevenagel reactions over modified basic microporous titanasilicate ETS-10

Yasuhide Goa,^a Peng Wu,^b and Takashi Tatsumi^{b,*}

^a Department of Applied Chemistry, Graduate School of Engineering, The University of Tokyo, 7-3-1, Hongo, Bunkyo-ku, Tokyo, 113-8656, Japan

^b Division of Materials Science & Chemical Engineering, Graduate School of Engineering, Yokohama National University, 79-5, Tokiwadai, Hodogaya-ku, Yokohama, Kanagawa, 240-8501, Japan

Received 15 December 2003; revised 14 January 2004; accepted 28 January 2004

Abstract

Al- and Ga-incorporated ETS-10, designated as ETAIS-10 and ETGaS-10, respectively, were synthesized by using P25 titania as a Ti source. The isomorphous substitution of Al and Ga for framework Si at the (4Si) environment was confirmed by ²⁹Si MASNMR measurements. ETS-10 was more active in the Knoevenagel condensation than Y-type zeolites. The introduction of Al and Ga into ETS-10 enhanced the activity, due to the increase of the ion-exchange sites, which act as Brønsted base sites. The ion exchange of Na and K in ETS-10 for larger alkali cations such as Rb or Cs caused an increase in the activity for the Knoevenagel reaction of the less reactive and less bulky substrates. ETS-10 selectively promoted the Knoevenagel condensation product compared to homogeneous amine catalysts, which produced the undesired self-condensed products of active methylene compounds.

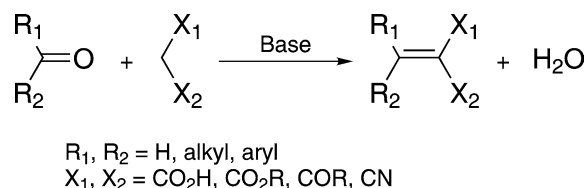
© 2004 Elsevier Inc. All rights reserved.

Keywords: ETS-10 titanasilicate; Isomorphous substitution; Ion exchange; Basicity; Knoevenagel condensation

1. Introduction

Conventional organic syntheses are generally based on homogeneous catalysts. In base-catalyzed reactions, organic amine, alkali alkoxide, and alkali hydroxide are widely used. However, these homogeneous reactions suffer disadvantages in separation, regeneration, etc. From the viewpoint of green chemistry, the use of heterogeneous catalysts is urgently desirable. Thus basic catalysis of inorganic solid materials has attracted intense interest as compiled in recent reviews [1–4].

The Knoevenagel condensation (Scheme 1) is a C=C double bond formation reaction between carbonyl compounds and active methylene compounds and widely employed to synthesize intermediates of fine chemicals. Conventionally, this reaction is catalyzed by weak bases like primary, secondary, tertiary amines, etc., under homogeneous conditions. Over the last decades, various solid catalysts and solid-supported catalysts have been applied to this reaction such as anion-exchange resin [5], KF [6], magnesium and aluminum oxides [7–9], alkali-exchanged and alkali-



Scheme 1. Base-catalyzed Knoevenagel condensation.

encapsulated zeolites [10–12], hydrotalcites [13], amino group-immobilized silica materials [14,15], clays [16], alkali and alkaline earth carbonates [17], nitridated aluminosilicates and aluminophosphates [18], and porous silicate-quaternary ammonium composites [19].

ETS-10 is one of the titanosilicates, first developed by Kuznicki [20]. ETS-10 has an ideal chemical formula of $\text{M}_{2/n}\text{Si}_5\text{TiO}_{13}$, where M represents a cation with a charge of plus n , and a quite unique structure in which semistraight Ti–O–Ti chains consisting of corner-sharing octahedral $[\text{TiO}_6]$ species run along (100) and (010) directions without intersections [21,22]. Owing to this nature, every $[\text{TiO}_6]$ tetrahedron of ETS-10 has two minus charges, making ETS-10 possess an ion-exchange capacity almost as high as zeolite Y with $\text{Si}/\text{Al} = 2.3$. Thus ETS-10 has a potential application

* Corresponding author.

E-mail address: ttatsumi@ynu.ac.jp (T. Tatsumi).

to cation-exchange agents, adsorbents, and acid-base catalysts. The three-dimensionally accessible 12-membered ring (12-MR) channel system of ETS-10 shows great promise as a catalyst for reaction involving bulky substances. Furthermore, the ion-exchange capacity can be controlled by isomorphously substituting Al^{3+} or Ga^{3+} for framework Si^{4+} atoms [23,24]. Philippou et al. have reported a number of gas-phase reactions catalyzed by base sites of ETS-10; dehydration of *tert*-butyl alcohol to *i*-butene [25], dehydrogenation of 2-propanol to acetone [26], and aldol condensation of acetone [27].

In this paper, we report the liquid-phase Knoevenagel reaction over ETS-10 and modified ETS-10 catalysts.

2. Experimental

2.1. Preparation of materials

ETS-10 was hydrothermally synthesized according to Liu and Thomas [28]. The introduction of trivalent cations of Al and Ga was conducted by adding the corresponding metal source to the synthesis gel. In a typical synthesis procedure, P25 titania (Nippon Aerosil) was dispersed in the aqueous solution of sodium hydroxide (Wako) and potassium fluoride (Nacalai). The hetero atom source, sodium aluminate (Nacalai) or gallium nitrate (Wako), was added and the mixture was stirred for 1 h. Then Ludox TM-40 colloidal silica (40 wt% in water, Aldrich) was added into the above suspension. After vigorous stirring for 2 h, the resulting white opaque silica–titania hydrogel was moved to a PTFE-lined stainless-steel autoclave and was hydrothermally crystallized at 473 K for 45 h. The chemical composition of the mother gel was adjusted to $5\text{SiO}_2 \cdot \text{TiO}_2 \cdot a\text{M}_2\text{O}_3 \cdot 3\text{NaOH} \cdot \text{KF} \cdot 75\text{H}_2\text{O}$, where M was Al or Ga and a was varied in the range of 0–0.15. After the synthesis, the solid product was centrifuged and well washed with deionized water until the pH of the top clear layer became below 10. The product was dried at 373 K overnight and finally calcined in air at 723 K for 6 h.

The ion-exchange treatment of ETS-10 with alkali salts was performed using 0.25 mol dm^{-3} aqueous solution of lithium nitrate (Wako), potassium nitrate (Koso), rubidium nitrate (Kishida), or cesium nitrate (Wako) at room temperature for 16 h. After the treatment, the sample was well washed, dried at 373 K for 2 h, and calcined at 723 K for 6 h.

NaY zeolite (SK-40) was purchased from Nikka Seiko Co., Ltd. The framework Si/Al atomic ratio was estimated to be 2.3 by the ^{29}Si MASNMR measurement.

2.2. Characterization

Powder X-ray diffractograms were obtained on a MAC Science MX-Labo diffractometer. The ^{29}Si , ^{27}Al , and ^{71}Ga MASNMR spectra were recorded on a JEOL ECA-400

Table 1
Measurement conditions of ^{29}Si , ^{27}Al , and ^{71}Ga MASNMR spectroscopy

| Nuclear | ^{29}Si | ^{27}Al | ^{71}Ga |
|---------------------------------|------------------|------------------|------------------|
| Magnetic field (MHz) | 79.6 | 104 | 122 |
| Magic angle spinning rate (kHz) | 5 | 10 | 9 |
| Recycle delay (s) | 15 | 2.0 | 2.0 |
| Pulse flip angle (deg) | 45 | 20 | 20 |

multinuclear solid-state magnetic resonance spectrometer. The conditions of the NMR measurements are listed in Table 1. Nitrogen adsorption analyses at 77 K were performed on a BEL Japan Belsorp 28SA automatic gas sorption meter. High-resolution argon adsorption isotherms were recorded on a Quantachrome Autosorb-1 apparatus at 87 K. Micropore-size distributions were calculated by the Saito–Foley (SF) method using Ar adsorption isotherms in the p/p_0 range of 10^{-6} – 10^{-1} [29,30]. Elemental analyses were conducted on a Shimadzu ICPS-8000E inductive coupled plasma-atomic emission spectrometer (ICP-AES). FT-IR spectra [31] of pyrrole-adsorbed samples were collected on a Perkin Elmer 1600 Series spectrometer. A self-supported wafer ($\sim 30 \text{ mg}$, $20 \text{ mm } \phi$) was evacuated in a quartz cell at 723 K for 3 h to desorb the water and was exposed to pyrrole vapor at room temperature for 5 min. IR spectra were recorded at room temperature.

2.3. Catalytic tests

The Knoevenagel reaction in the liquid-phase was employed as a test reaction. All the catalytic reactions were conducted batchwise in a water-bathed 25 cm^3 round-bottom flask equipped with a Dimroth condenser. The reaction mixture was continuously stirred with a magnetic stirrer. After the reaction, the flask was quenched with ice water and the liquid phase was collected after the separation by centrifugation. Quantitative analyses of the products were performed on a Shimadzu GC-14B gas chromatograph equipped with a 50 m OV-1 capillary column and a hydrogen flame-ionization detector using *n*-decane as an internal standard.

Two types of Knoevenagel reactions were performed. For reaction **1** to form ethyl α -cyanocinnamate (ECC), 10 mmol of benzaldehyde (BA), 10 mmol of ethyl cyanoacetate (ECA), 15 cm^3 of ethanol as a solvent, and 30 mg of catalyst were mixed and heated to 323 K for 2 h. Reaction **2** to form 1,1-dicyano-2-methylpropene (DCMP) was conducted by mixing 20 cm^3 of acetone (275 mmol), 10 mmol of malononitrile (MN), and 20 mg of catalyst at 313 K for 0.5 h.

3. Results and discussion

3.1. Characterization of the synthesized materials

Powder XRD patterns of the materials are illustrated in Fig. 1. When neither Al nor Ga were added, pure ETS-10 was obtained. The addition of Al or Ga in the synthesis gel

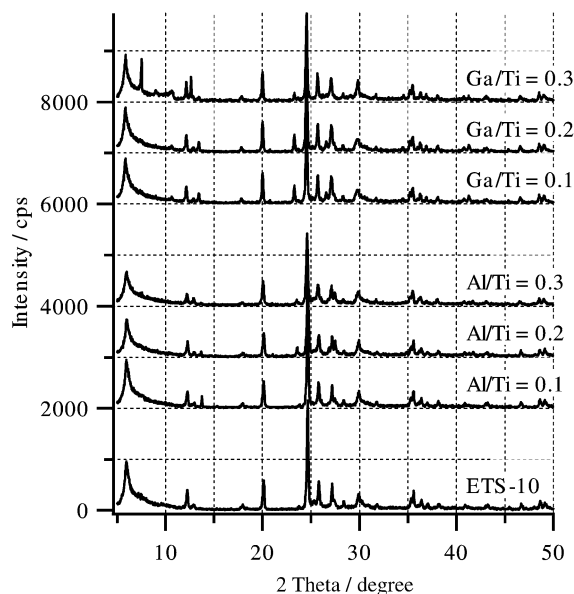


Fig. 1. XRD patterns of as-synthesized Al- and Ga-introduced [Na, K]-ETS-10 titanosilicates.

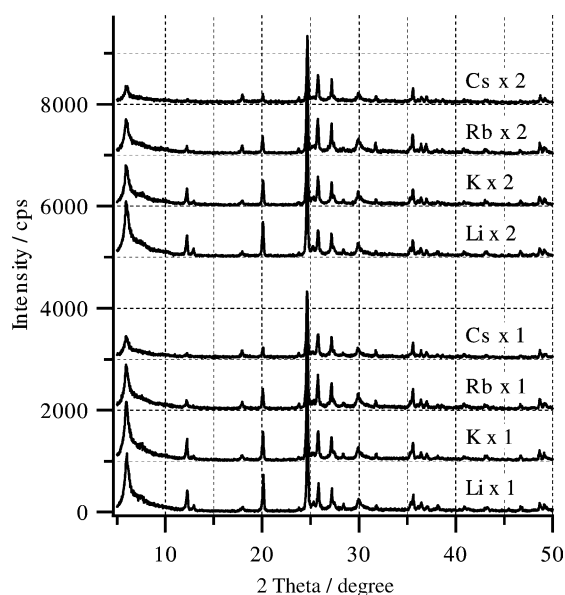


Fig. 2. XRD patterns of alkali-exchanged ETS-10 titanosilicates.

gave rise to a slight decrease in the crystallinity of ETS-10 and the coproduction of the impurity such as ETS-4, α -quartz, and anatase. The formation of the impurity increased with an increasing amount of Al or Ga added. However, the main phase obtained was ETS-10 in the range of Al/Ti or Ga/Ti ratio examined in this study.

Fig. 2 shows the XRD patterns of alkali-exchanged ETS-10 titanosilicates. Compared to the original ETS-10 (Fig. 1), the diffraction peaks of the Li-exchanged sample increased in intensity and those of the Rb- and Cs-exchanged samples decreased. The main reason is probably not the decrease of the crystallinity but the scattering effects of introduced alkali metal cations on X-ray. Anderson et al. proposed that

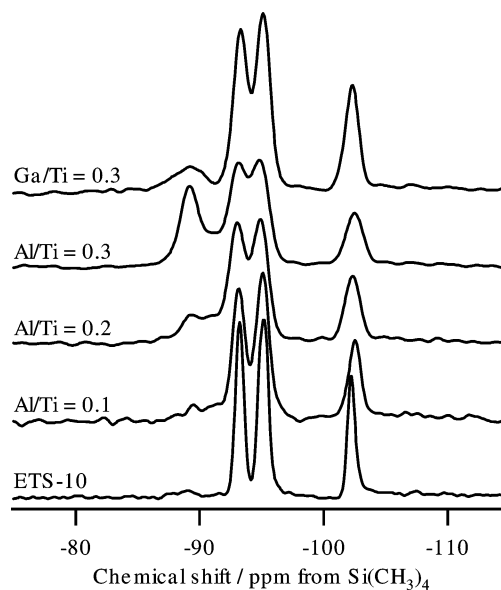


Fig. 3. ^{29}Si MASNMR spectra of Al- and Ga-introduced [Na, K]-ETS-10 titanosilicates.

there are five cations sites in ETS-10 [32]. The ion exchange would not occur site selectively, which could result in the random distribution of electron in the ion-exchanged ETS-10 samples. Rb- and Cs-exchanged ETS-10 samples contain a larger number of randomly distributed electrons. The more randomly electrons distribute, the more X-ray photons are scattered to decrease the diffraction peaks in intensity. The second ion-exchange treatments caused the decrease in the diffraction intensity for all the samples. Repeated thermal treatments might have given rise to the slight degradation of the ETS-10 structure.

^{29}Si MASNMR spectra are shown in Fig. 3. Three well-resolved peaks were observed for the ETS-10 sample; two peaks at -93.2 and -95.1 ppm and a peak at -102.2 ppm are attributed to Si atoms at (3Si, 1Ti) and (4Si) environments, respectively. The introduction of Al or Ga into ETS-10 led to the appearance of a new peak around -89 ppm assigned to Si atoms at (2Si, 1Ti, 1Al, or 1Ga), which indicated that the Al or Ga atoms were isomorphously substituted for Si atoms at (4Si) sites. The introduction of Al and Ga was accompanied by a peak broadening, due to the increased variation of the chemical environment around Si. The more Al atoms were introduced into the framework, the more the peaks broadened. Fig. 4 shows ^{27}Al MASNMR spectra of Al-introduced ETS-10 samples. Obviously almost all the Al atoms were located in the tetrahedral environment and a quite low amount of octahedrally coordinated Al was observed. These observations are consistent with those reported by Anderson et al. [24]. A ^{71}Ga MASNMR spectrum of Ga-introduced ETS-10 sample shown in Fig. 5 revealed the presence of octahedrally coordinated Ga species (~ 0 ppm) together with tetrahedrally coordinated Ga species (~ 180 ppm). Pentacoordinated Ga species might also be present in the sample (~ 80 ppm). These observa-

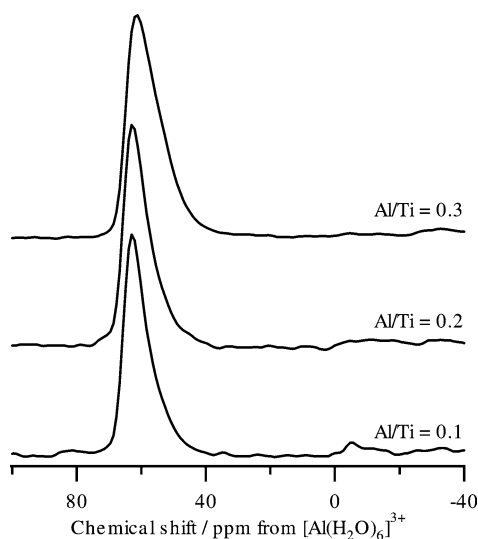


Fig. 4. ^{27}Al MASNMR spectra of Al-introduced [Na, K]-ETS-10 titanosilicates.

tions strongly indicate the presence of extraframework Ga species.

The intraframework and bulk silicon/metal ratios were determined by ^{29}Si MASNMR peak areas [24] and ICP-AES, respectively (Table 2). The ^{29}Si MASNMR spectra were deconvoluted into Gaussian functions. The Si/Ti ratio of pure ETS-10 was ca. 5. When Al or Ga was introduced into the ETS-10 structure, the framework Al/Ti or Ga/Ti ratio increased. In the case of Al-incorporated ETS-10, the framework Al/Ti ratio was comparable to the bulk Al/Ti ratio. The (Si + Al)/Ti ratio in the framework proved to be

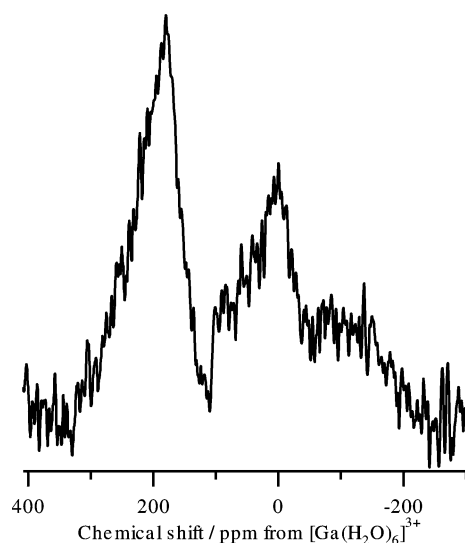


Fig. 5. A ^{71}Ga MASNMR spectrum of Ga-introduced [Na, K]-ETS-10 titanosilicate. Ga/Ti ratio in the synthesis gel was 0.3.

constantly 5, which could also evidence the isomorphous substitution of Al for Si. On the other hand, the framework Ga/Ti ratio of ETGaS-10 was about half of the bulk Ga/Ti ratio, being consistent with the result of ^{71}Ga MASNMR spectroscopy which indicated the presence of the extraframework Ga species.

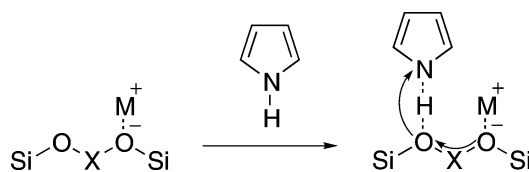
3.2. Estimation of the base strength

Weakly acidic pyrrole can be used as a probe for the evaluation of basicity of the solid. The IR band attributed to the

Table 2

Results of peak deconvolution of ^{29}Si MASNMR and calculated Si/metal ratios of Al- and Ga-introduced ETS-10 materials

| Introduced metal | Chemical environment | Chemical shift (ppm) | Relative intensity | FWHM (ppm) | Intraframework | | | Bulk metal/Ti |
|------------------|----------------------|----------------------|--------------------|------------|----------------|----------|-----------------|---------------|
| | | | | | Si/Ti | Metal/Ti | (Si + Metal)/Ti | |
| None | (4Si) | -102.3 | 1.000 | 0.443 | 5.04 | - | 5.04 | - |
| | (3Si, 1Ti) | -95.1 | 1.560 | 0.592 | | | | |
| | (3Si, 1Ti) | -93.2 | 1.502 | 0.515 | | | | |
| Al (0.1) | (4Si) | -102.2 | 1.000 | 0.768 | 5.00 | 0.11 | 5.11 | 0.10 |
| | (3Si, 1Ti) | -94.8 | 1.887 | 0.798 | | | | |
| | (3Si, 1Ti) | -92.8 | 1.708 | 0.721 | | | | |
| | (2Si, 1Ti, 1Al) | -91.1 | 0.192 | 0.917 | | | | |
| | (2Si, 1Ti, 1Al) | -89.2 | 0.160 | 1.063 | | | | |
| Al (0.2) | (4Si) | -102.0 | 1.000 | 0.909 | 4.87 | 0.19 | 5.06 | 0.22 |
| | (3Si, 1Ti) | -94.6 | 1.852 | 0.918 | | | | |
| | (3Si, 1Ti) | -92.7 | 1.797 | 0.928 | | | | |
| | (2Si, 1Ti, 1Al) | -90.9 | 0.264 | 0.803 | | | | |
| | (2Si, 1Ti, 1Al) | -89.2 | 0.403 | 1.485 | | | | |
| Al (0.3) | (4Si) | -102.2 | 1.000 | 1.040 | 4.81 | 0.26 | 5.07 | 0.28 |
| | (3Si, 1Ti) | -94.6 | 1.986 | 1.039 | | | | |
| | (3Si, 1Ti) | -92.8 | 1.886 | 0.987 | | | | |
| | (2Si, 1Ti, 1Al) | -90.6 | 0.518 | 0.901 | | | | |
| | (2Si, 1Ti, 1Al) | -88.9 | 1.507 | 1.145 | | | | |
| Ga (0.3) | (4Si) | -102.3 | 1.000 | 0.802 | 5.03 | 0.13 | 5.16 | 0.25 |
| | (3Si, 1Ti) | -95.1 | 1.723 | 0.820 | | | | |
| | (3Si, 1Ti) | -93.3 | 1.539 | 0.840 | | | | |
| | (2Si, 1Ti, 1Ga) | -89.2 | 0.213 | 1.953 | | | | |



Scheme 2. Model for pyrrole chemisorbed on a basic site. M and X represent an ion-exchangeable alkali metal cation and framework Ti, Al, or Ga atom, respectively.

Table 3
Shifts of N–H vibration of pyrrole adsorbed on alkali-exchanged Y and ETS-10 materials

| Catalyst | Na/Ti | K/Ti | Metal/Ti | $\Delta\nu_{\text{NH}}$ (cm^{-1}) |
|----------------|-------------------|------|-------------------|--|
| Li–Y | 0.36 ^a | | 0.64 ^b | Not resolved |
| Na–Y | 1.00 ^a | | – | 37 |
| Cs–Y | 0.55 ^a | | 0.45 ^b | 110, 40 |
| Li–ETS-10 | 1.18 | 0.39 | 0.45 | Not resolved |
| [Na, K]–ETS-10 | 1.51 | 0.47 | – | 90 |
| Cs–ETS-10 | 1.25 | 0.41 | 0.30 | 190, 90 |

^a Na/Al ratio.

^b Metal/Al ratio.

N–H stretching vibration shifts to a lower wavenumber on the interaction of the H atom of pyrrole with a Brønsted base site (Scheme 2). Barthomeuf measured the shifts of N–H vibration of pyrrole adsorbed on alkali-exchanged zeolites and verified that the shift was a function of the basicity [2,31]. The results of the pyrrole IR are summarized in Table 3. The shift of the N–H absorption band, $\Delta\nu_{\text{N–H}}$, of Na–Y was 37 cm^{-1} . After the ion-exchange treatment of Na–Y with Cs, a new band at $\Delta\nu_{\text{N–H}} = 110 \text{ cm}^{-1}$ appeared, indicating the generation of stronger Brønsted base sites. When [Na, K]–ETS-10 was treated with a Cs solution, a band at $\Delta\nu_{\text{N–H}} = 190 \text{ cm}^{-1}$ was observed in addition to the original band at $\Delta\nu_{\text{N–H}} = 90 \text{ cm}^{-1}$. The larger $\Delta\nu_{\text{N–H}}$ observed on Cs–ETS-10 than that on Cs–Y suggests the stronger basicity of Cs–ETS-10 than Cs–Y.

The electronegativity of Ti is slightly lower than that of Al. Moreover, two minus charges are shared by surrounding six oxygen atoms of $[\text{TiO}_6]$ octahedra in ETS-10 materials, while one minus charge is shared by four oxygen atoms of $[\text{AlO}_4]$ in Y zeolite. The electron density of oxygen atom around Ti in ETS-10 is higher than that around Al in Y zeolite, resulting in the larger shift of $\Delta\nu_{\text{N–H}}$, indicating the stronger basicity of ETS-10 than Y zeolite.

3.3. Knoevenagel condensation

3.3.1. Knoevenagel condensation between benzaldehyde and ethyl cyanoacetate

Table 4 shows the activity of various solid-base catalysts for the Knoevenagel reaction. When benzaldehyde and ethyl cyanoacetate were used as substrates, ETS-10 gave a higher yield of ethyl α -cyanoacetate (**1**) than Na–Y zeolite. Al and Ga introduction into ETS-10 (ETAIS-10 and ETGaS-10, respectively) increased the yield of ECC, probably due to the

Table 4
The results of Knoevenagel reaction between carbonyl compounds and active methylene compounds^a

| Run | Catalyst | Yield ^b (mol%) | |
|-----|------------------------|--|--|
| | | 1: $\text{R}_1 = \text{H}, \text{R}_2 = \text{Ph}, \text{X} = \text{CO}_2\text{C}_2\text{H}_5$ | 2: $\text{R}_1 = \text{R}_2 = \text{CH}_3, \text{X} = \text{CN}$ |
| 1 | [Na,K]–ETS-10 | 28.8 | 23.0 |
| 2 | ETAIS-10 | 38.4 | 37.0 |
| 3 | ETGaS-10 | 41.5 | 41.0 |
| 4 | Li–ETS-10 | 44.3 | 14.2 |
| 5 | K–ETS-10 | 31.5 | 25.0 |
| 6 | Rb–ETS-10 | 33.3 | 28.3 |
| 7 | Cs–ETS-10 | 32.7 | 27.7 |
| 8 | Li–ETS-10 ^c | n.d. ^d | 7.1 |
| 9 | K–ETS-10 ^c | n.d. ^d | 24.9 |
| 10 | Rb–ETS-10 ^c | n.d. ^d | 21.0 |
| 11 | Cs–ETS-10 ^c | n.d. ^d | 22.8 |
| 12 | Na–Y | 14.5 | 0.0 |
| 13 | Li–Y | 10.7 | 0.0 |
| 14 | K–Y | 9.4 | 0.0 |
| 15 | Rb–Y | 5.2 | 0.0 |
| 16 | Cs–Y | 6.6 | 0.0 |
| 17 | None | 3.3 | 0.0 |
| 18 | JRC-MGO-4-500A | 78.2 | 3.8 |

^a Reaction conditions: for reaction **1**, time, 2 h; temperature, 323 K; 15 cm^3 of ethanol as solvent, 5 mmol of benzaldehyde, 5 mmol of ethyl cyanoacetate, and 30 mg of catalyst; for reaction **2**, time, 0.5 h; temperature, 313 K; 20 cm^3 of acetone, 10 mmol of malononitrile, and 20 mg of catalyst.

^b No by-products other than the Knoevenagel condensation products were obtained.

^c The twice ion-exchanged materials were used as catalysts. Li/Ti = 0.65, Cs/Ti = 0.42. K/Ti and Rb/Ti were not determined.

^d Not determined.

increase in the ion-exchange sites leading to the increase in the catalytically active Brønsted base sites. Ti–O–Ti chains face the 7-MR channels of ETS-10 but not the 12-MR channels, while Al and Ga atoms substitute the intraframework (4Si) sites facing 12-MR channels. Although a relatively small amount of Al or Ga was introduced into the ETS-10 framework compared to the Ti amount, the ion-exchange sites originating from the framework Al or Ga existed on the main channels efficiently and then enhanced the catalytic activity.

The ion-exchange treatment of original [Na, K]–ETS-10 with various alkali metal salts caused the change of the catalytic properties of ETS-10 materials; Li increased and Cs decreased the yield of ECC. Similar results were obtained when alkali-exchanged Y zeolites were used as catalysts. This is contrary to what was reported for the effect of ion exchange of X and Y zeolites; heavier alkali metal cation-exchanged X and Y zeolites exhibit higher basicity [10]. The molecular size of ECC is estimated to be ca. $12 \times 6 \text{ \AA}^2$. Since Rb and Cs decreased the effective pore diameter of ETS-10 in contrast to Li, the narrowed channels could impose serious restriction on the formation and/or diffusion of ECC

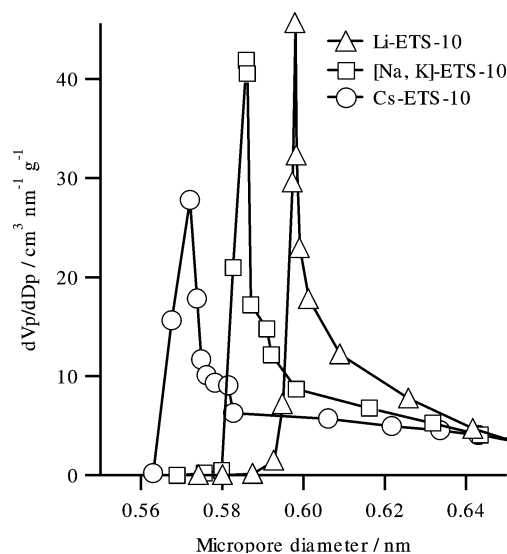


Fig. 6. Micropore-size distributions of original [Na, K]-ETS-10 and Li- and Cs-exchanged ETS-10 titanosilicates.

Table 5

Surface area and micropore volume of alkali-exchanged ETS-10 materials

| Catalyst | A_{Lang}^a ($\text{m}^2 \text{g}^{-1}$) | V_p^b ($\text{mm}^3 \text{g}^{-1}$) |
|----------------|--|---|
| [Na, K]-ETS-10 | 401 | 104 |
| Li-ETS-10 | 391 | 122 |
| K-ETS-10 | 388 | 87 |
| Rb-ETS-10 | 339 | 85 |
| Cs-ETS-10 | 290 | 73 |

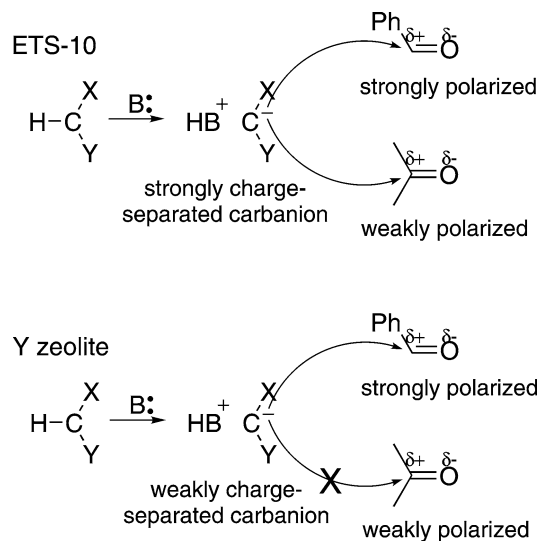
^a Langmuir surface area.

^b Micropore volume calculated by the t plot.

molecules. The highest yield of ECC was obtained over nonporous magnesia catalysts with extremely small crystal sizes (JRC-MGO-4-500A, average crystal size = 50 nm, BET surface area $\sim 30 \text{ m}^2 \text{g}^{-1}$).

Micropore-size distributions of original [Na, K]-ETS-10 and Li- and Cs-exchanged ETS-10 are shown in Fig. 6. The micropore size decreased in the order of Li-ETS-10 > [Na, K]-ETS-10 > Cs-ETS-10. As shown in Table 5, the micropore volume and Langmuir surface area obviously decreased with increasing size of the cations. Minor structural degradation or pore blocking might have occurred during the ion-exchange treatment with Rb or Cs, resulting in the reduced microporosity of the ETS-10 materials.

Knoevenagel condensation between BA and ECA is a facile reaction since the carbonyl group of BA is attached to only one mildly electron-donating group (Ph-) which slightly decreases the positive charge on the C atom of the carbonyl group. Even without any catalyst, the condensation proceeded to give the ECC yield of 3.8%. The basicity of ETS-10 and also Y zeolite might be too strong to discuss the relationship between the basicity and the activity for this reaction (Scheme 3). The yield of ECC would be simply dependent on the accessibility of the substrates to the base sites of the catalyst.



Scheme 3. The relationship between the base strength and the reactivity of the carbanion generated on the base site.

3.3.2. Knoevenagel condensation between acetone and malononitrile

In order to investigate the catalytic ability of ETS-10 for the reactions demanding less reaction space, smaller substrates giving a smaller condensed product were employed. The yield of the Knoevenagel reaction product from acetone and malononitrile (MN) is also listed in Table 4. The condensed product, 1,1-dicyano-2-methylpropene (**2**), was hardly obtained over nonporous magnesia and Y-type zeolite. Since the carbonyl group of acetone has two electron-donating groups (CH_3-), which could increase a steric hindrance around the carbonyl carbon and decrease the $\delta+$ charge on the C atom of the carbonyl group, the condensation between acetone and MN would need a stronger base, which would increase the degree of the charge separation of the carbanion and the protonated base pair. The basicity of Y-type zeolites, even Cs-Y, and magnesia was not strong enough for the production of DCMP (Scheme 3). In contrast, ETS-10 efficiently catalyzed the condensation of acetone and MN even at a mild temperature of 313 K, due to its stronger basicity (Scheme 3). In a similar manner to the condensation of BA and ECA to form ECC, the introduction of Al or Ga into the framework of ETS-10 increased the yield of DCMP, which can also be attributed to an increase in the ion-exchange sites on the 12-MR channels.

The activity of alkali-exchanged ETS-10 increased in the following order: Li < [Na, K] < K < Rb \approx Cs, which is consistent with the previous observations in the Knoevenagel condensation between BA and ECA over alkali-exchanged X and Y-type zeolites by Corma et al. [10]. The condensation between acetone and MN should need a stronger basicity than that between BA and ECA because of the lower positive charge on the C atom of the carbonyl group and steric hindrance induced by the two methyl substituents. The stronger Brønsted basicity of ETS-10 more strongly separated the charge between the protonated base site and the carbanion

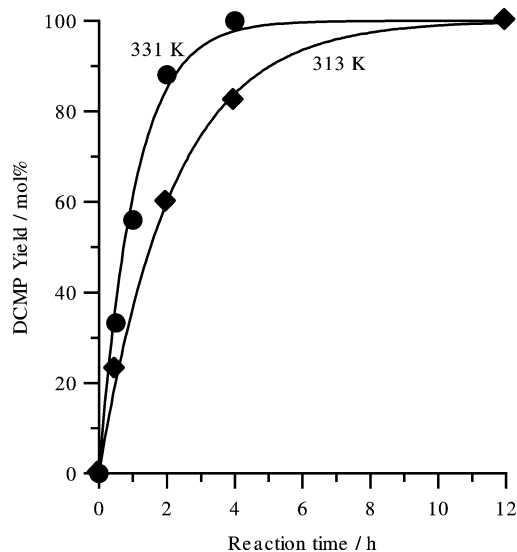


Fig. 7. Time course of the Knoevenagel condensation between acetone and MN. Reaction conditions: temperature, 313 and 331 K; time, 0.5–12 h; 20 cm³ of acetone, 10 mmol of malononitrile, and 20 mg of [Na, K]-ETS-10.

generated from MN, which assisted the nucleophilic attack to the more weakly polarized carbonyl groups.

As shown in Table 4, after the second alkali exchange of the once exchanged ETS-10 catalysts, a lowered yield of DCMP was observed in all cases. The lowered activity of Li-exchanged ETS-10 is due to the lowered basicity. We suppose that the increased amount of Rb or Cs ions introduced by the second exchange would prevent the access of the substrate molecules to the active sites even in the reaction between acetone and MN.

It could be noteworthy that the selectivity to the Knoevenagel condensation products (both **1** and **2**) was 100% over all of the catalysts shown in Table 3.

3.3.3. Effect of the reaction time, temperature, and catalyst weight

Fig. 7 shows the effect of the reaction time and temperature on the formation of DCMP catalyzed by [Na, K]-ETS-10. The yield of DCMP reached 100% after 12 and 4 h at temperatures of 313 K and 331 K, respectively. The reaction proceeded in the pseudo-first order of MN because an excess amount of the other substrate, acetone, existed in the reaction system. The initial turnover frequencies were found to be 51.9 and 99.3 mol (mol-ion-exchange sites)⁻¹ h⁻¹ at 313 and 331 K, respectively. When 100 mg catalyst was used, DCMP was obtained at 93% at 313 K after 0.5 h reaction time (Fig. 8), indicating that the condensation between acetone and MN proceeded very efficiently under mild conditions.

3.3.4. A comparison with organic amine catalyst

The Knoevenagel reaction is conventionally catalyzed by organic bases. We made a comparison of the catalytic properties between [Na, K]-ETS-10 and homogeneous base cat-

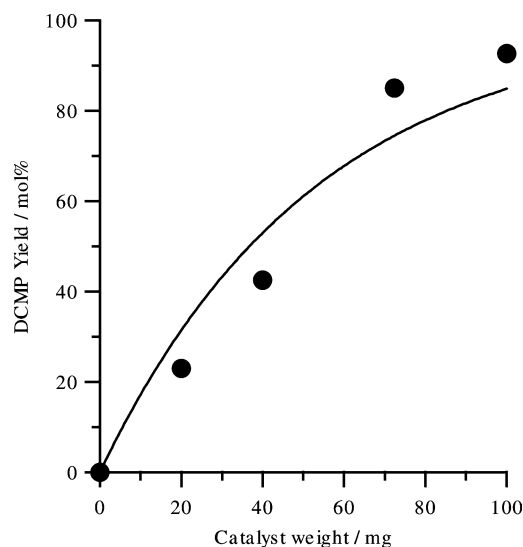


Fig. 8. The effect of the catalyst weight. Reaction conditions: temperature, 313 K; time, 0.5 h; 20 cm³ of acetone, 10 mmol of malononitrile, and 20–100 mg of [Na, K]-ETS-10.

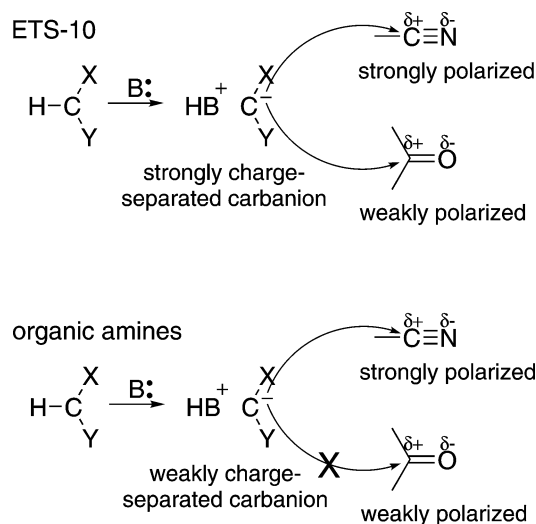
Table 6
The comparison of ETS-10 and the organic amines^a

| Run | Catalyst | Conversion (mol%) | Selectivity (mol%) | |
|-----|----------------|-------------------|--------------------|--------|
| | | | DCMP | Others |
| 1 | [Na, K]-ETS-10 | 23.0 | 100 | 0 |
| 2 | Piperidine | > 99 | 16 | 84 |
| 3 | Triethylamine | > 99 | 56 | 44 |

^a Reaction conditions: time, 0.5 h; temperature, 313 K; 20 cm³ of acetone, 10 mmol of malononitrile, and 20 mg of ETS-10 or 90 μmol of amines.

alysts. The results are shown in Table 6. The amount of the organic base catalyst was adjusted to 90 μmol, corresponding to the amount of the ion-exchange sites in 20 mg of [Na, K]-ETS-10. [Na, K]-ETS-10 exhibited 100% selectivity for the Knoevenagel condensation product with no by-products; however, piperidine and triethylamine gave low selectivity to the Knoevenagel condensation product; instead the self-condensation of MN mainly occurred. The carbanions generated by the deprotonation of MN with piperidine or pyridine did not attack the carbonyl group of acetone but the cyano group of MN predominantly.

The mechanism of the selective reaction on ETS-10 is shown in Scheme 4. The polarizability of the C–H bond of the intermediate generated from the Brønsted base site of ETS-10 and MN could be larger than that generated from organic amine and MN. The carbonyl carbon of acetone is charged less positively than the cyano carbon of MN. The strongly polarized intermediate more easily attacks the carbonyl carbon of acetone which is less positively charged than the cyano carbon of MN. Since much more acetone than MN exists in the reaction mixture (acetone/MN molar ratio = 27.5), the Knoevenagel condensation occurred prior to the self-condensation of MN.



Scheme 4. The comparison of the base strength of ETS-10 and organic amines.

3.3.5. Recyclability of the catalyst

We also examined the recyclability of the [Na, K]-ETS-10 catalyst. Here, reaction 1 was employed as the test reaction. The used catalyst was calcined at 723 K for 6 h. After the third regeneration, 27.3% yield of ECC was obtained, indicating that ETS-10 is a recyclable solid-base catalyst.

4. Conclusions

Al and Ga were successfully incorporated into the framework of ETS-10, isomorphously replacing the (4Si) sites. While no extraframework Al species were detected by ^{27}Al MASNMR measurements, about half of Ga introduced existed out of the framework. Na^+ and K^+ of the original [Na, K]-ETS-10 was ion-exchanged for various alkali metal cations. Pyrrole-IR spectroscopy showed that the basicity of Cs-ETS-10 was stronger than that of Cs-Y. For the Knoevenagel condensation between benzaldehyde and ethyl cyanoacetate, Cs-exchanged ETS-10 exhibited a lower activity than the original [Na, K]-ETS-10. This is probably because of the narrowed reaction space in the catalyst due to the presence of the cations large size. In contrast, the ion exchange with Li increased the activity. When the condensation between acetone and malononitrile, which needs a stronger basicity, was employed as a probe reaction, Cs-exchanged ETS-10 exhibited high activity. ETS-10 catalyzed the condensation between acetone and malononitrile selectively, while organic amine such as piperidine and triethylamine produced the self-condensed products of malononitrile. The Knoevenagel condensation product was quantitatively obtained after 12 h at 313 K and after 4 h at 331 K over [Na, K]-ETS-10. These findings indicate that

ETS-10 is effective in the heterogeneous base-catalyzed reaction for the production of fine chemicals involving small size substances.

Acknowledgments

The authors thank Prof. T. Meguro and Mr. T. Amaoka for the measurements and the fruitful discussion on Ar adsorption.

References

- [1] H. Hattori, Appl. Catal. A 222 (2001) 247.
- [2] H. Hattori, Chem. Rev. 95 (1995) 537.
- [3] R.J. Davis, J. Catal. 216 (2003) 396.
- [4] Y. Ono, J. Catal. 216 (2003) 406.
- [5] W. Richardhein, J. Melvin, J. Org. Chem. 26 (1961) 4874.
- [6] L. Rand, D. Haidukewych, R.J. Dolinski, J. Org. Chem. 31 (1966) 1272.
- [7] H. Moison, F. Texier-Boulet, A. Foucaud, Tetrahedron 43 (1987) 537.
- [8] J. Muzart, Synthesis (1982) 60.
- [9] F. Texier-Boulet, A. Foucaud, Tetrahedron Lett. 23 (1982) 4927.
- [10] A. Corma, V. Fornés, R.M. Martín-Aranda, H. García, J. Primo, Appl. Catal. 59 (1990) 237.
- [11] I. Rodríguez, H. Cambon, D. Brunel, M. Laspéras, J. Mol. Catal. A 130 (1998) 195.
- [12] C.F. Linares, M.R. Goldwasser, F.J. Machado, R. Aramis, G. Rodríguez-Fuentes, J. Barrault, Micropor. Mesopor. Mater. 41 (2000) 69.
- [13] A. Corma, V. Fornés, R.M. Martín-Aranda, F. Rey, J. Catal. 134 (1992) 58.
- [14] E. Angeletti, C. Canepa, G. Martinetti, P. Venturello, J. Chem. Soc., Perkin Trans. 1 (1989) 105.
- [15] B.M. Choudary, M.L. Kantam, P. Sreekanth, T. Bandopadhyay, F. Figueras, A. Tuel, J. Mol. Catal. A 142 (1999) 361.
- [16] Y.V. Subba Rao, B.M. Choudary, Synth. Commun. 21 (1991) 1163.
- [17] M.A. Aramendia, V. Borau, C. Jimenez, J.M. Marinas, F.J. Romero, Chem. Lett. (1995) 279.
- [18] S. Ernst, M. Hartmann, S. Sauerbeck, T. Bongers, Appl. Catal. A 200 (2000) 117.
- [19] Y. Kubota, Y. Nishizaki, Y. Sugi, Chem. Lett. (2000) 998.
- [20] S.M. Kuznicki, US patent 4,853,202, 1989.
- [21] M.W. Anderson, O. Terasaki, T. Ohsuna, A. Philippou, S.P. MacKay, A. Ferreira, J. Rocha, S. Lidin, Nature 367 (1994) 347.
- [22] M.W. Anderson, O. Terasaki, T. Ohsuna, P.J.O. Malley, A. Philippou, S.P. MacKay, A. Ferreira, J. Rocha, S. Lidin, Philos. Mag. B 71 (1995) 813.
- [23] S.M. Kuznicki, K.A. Thrush, US patent 5,244,650, 1993.
- [24] M.W. Anderson, J. Rocha, Z. Lin, A. Philippou, I. Orion, A. Ferreira, Micropor. Mater. 6 (1996) 195.
- [25] A. Philippou, M. Naderi, J. Rocha, M.W. Anderson, Catal. Lett. 53 (1998) 221.
- [26] A. Philippou, J. Rocha, M.W. Anderson, Catal. Lett. 57 (1999) 151.
- [27] A. Philippou, M.W. Anderson, J. Catal. 189 (2000) 395.
- [28] X. Liu, J.K. Thomas, Chem. Commun. (1996) 1435.
- [29] A. Saito, H.C. Foley, AIChE J. 37 (1991) 429.
- [30] A. Saito, H.C. Foley, Micropor. Mater. 3 (1995) 531.
- [31] D. Barthomeuf, J. Phys. Chem. 88 (1984) 42.
- [32] M.W. Anderson, J.R. Agger, D.-P. Luigi, A.K. Baggaley, J. Rocha, Phys. Chem. Chem. Phys. 1 (1999) 2287.